Fibers and Polymers 2012, Vol.13, No.3, 339-345 DOI 10.1007/s12221-012-0339-x

Preparation and Characterization of (polyurethane/nylon-6) Nanofiber/(silicone) Film Composites *via* Electrospinning and Dip-coating

Chan-Hee Park[1†], Chae-Hwa Kim[1†], Leonard D. Tijing[2], Do-Hee Lee[1], Mi-Hwa Yu[1], Hem Raj Pant[1,3], Yonjig Kim[2], and Cheol Sang Kim[1,2*]

[1]*Department of Bionanosystem Engineering, Chonbuk National University, Jeonju 561-756, Korea*
[2]*Division of Mechanical Design Engineering, Chonbuk National University, Jeonju 561-756, Korea*
[3]*Institute of Engineering, Pulchowk Campus Tribhuvan University, Kathmandu, Nepal*
(Received July 25, 2011; Revised October 8, 2011; Accepted October 28, 2011)

Abstract: This paper reports on the preparation and characterization of nanofibers and nanofiber/film composites fabricated by electrospinning and dip-coating. The polymers in this study consist of polyurethane, nylon-6, and silicone. Scanning electron microscopy (SEM), fiber distribution, X-ray diffraction (XRD) analysis, Fourier transform infrared spectroscopy (FTIR) and tensile tests were conducted. The electrospun nylon-6 nanofiber/dip-coated silicone film (dried for 5 min) showed the optimum tensile strength and strain results, showing an increase in tensile strength of 63 % compared to pure nylon-6 nanofiber alone. XRD and FTIR verified the presence of individual polymers in the composite matrix. The electrospun PU nanofiber produced the biggest fiber diameter, while electrospun nylon-6, and PU/nylon-6 produced uniform fiber diameters, with PU/nylon-6 obtaining very random and curved fiber morphology.

Keywords: Electrospinning, Nanofiber, Dip-coating, Film, Polymers

Introduction

A non-vascular stent is a medical device that is used as an artificial scaffold to relieve obstructions inside the body with an advantage of minimal invasion [1,2]. But the use of bare non-vascular stents has an issue of re-occlusion of passageway due to tumor in-growth. Many studies [3-7] have been carried out on the use of polymeric films as cover for non-vascular stents in order to inhibit the overgrowth of smooth muscles, such as malignant tissues in bile duct cancer or esophageal cancer, which infiltrate the lumen and causes blockage in the passageway [3,4]. Some of the polymers used as cover film are polyurethane, silicone, salmon collagen, polytetrafluoroethylene (PTFE), polysaccharide-PTFE, and polyethylene terephthalate [4,8-10]. From among these polymers, commercialized non-vascular stents usually utilize silicone and polyurethane as cover film. The most common method used in fabricating stent cover is by dip-coating technique. In dip-coating, the stent is either immersed in a polymer solution or the polymer solution is applied to the stent placed on a rotating mandrel. The film covered non-vascular stents had some degree of success, but the continuous growth of tumors could eventually break the film cover, causing re-obstruction of the passageway [4]. Some polymers also elicit inflammatory reaction leading to restenosis [3]. Important factors for a continuous patency of non-vascular stent cover are biocompatibility, good tensile strength and flexibility, and high surface area for possible inclusion of drug coatings [3,4,6]. The stent cover must be able to withstand the force from crimping, insertion, and deployment of non-vascular stent to and from the catheter to avoid any damage to the film membrane. One way of improving the properties of a stent cover is by utilizing polymer nanofibers by electrospinning, which creates more surface area for attachment of drugs.

Electrospinning is an efficient and easy technique for the fabrication of polymeric nanofibers, which has many applications such as in tissue and biomedical engineering, filtration, clothing and textiles, and composite materials [11-19]. The nanometer-range diameters of electrospun fibers give them unique properties such as very large surface area to volume ratio, flexibility in surface functionalities, superior mechanical performance, high porosity, and good interfacial adhesion [20-25]. Single or blended polymer composites have been widely studied. Lin *et al*. [26] reported increased mechanical properties of their prepared composite material of PAN core-PMMA shell nanofiber reinforced Bis-GMA composite by electrospinning and resin molding. Recently, Liao and co-workers [23] prepared a nanofiber-reinforced epoxy composite film via electrospinning and solution-impregnation method. They reported strong interfacial adhesion for cellulose acetate (CA)/epoxy composites while less interfacial adhesion for polyurethane/epoxy composites. This strong interfacial adhesion leads to high mechanical strength of the resulting CA/epoxy composite film.

A challenge still remains on the production of suitable polymeric cover that would provide good tensile strength, and flexibility to maintain patency of stent covers. In line with this, our main goal in the present study was to develop a potential non-vascular stent cover with improved mechanical properties. Here, biocompatible silicone and poly-

†These authors contributed equally to this work.
*Corresponding author: chskim@jbnu.ac.kr

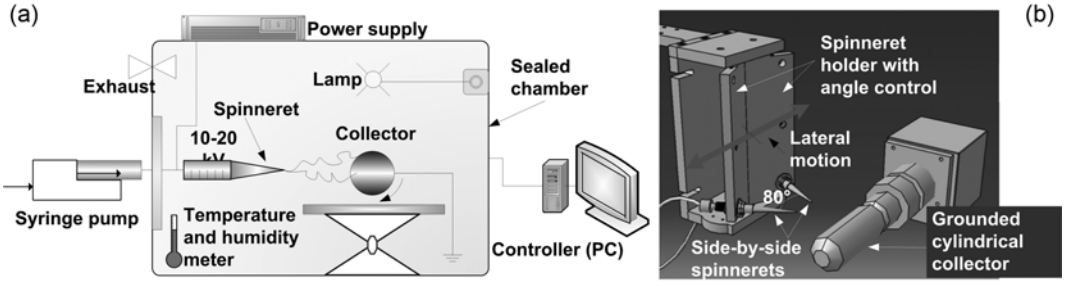

Figure 1. The present (a) single-nozzle electrospinning system and (b) side-by-side electrospinning configuration.

urethane were used as the main materials for making stent cover dip-coated films as they are commonly used as cover for commercial non-vascular stents. Silicone film has high flexibility but suffers from low tensile strength, while polyurethane film has very good tensile strength but is quite stiff. Thus, it is imperative that we improve the individual properties of these polymers by either incorporating some filler materials like nanofibers or by blending different polymers. To address the issue of restenosis, drug-eluting stents show a lot of promise [7]. The optimal design for drug-release in stent covers should have a large surface area-to-volume ratio so that there would be more area for drugs to attach. The best candidate for this would be electrospun nanofibers. So, we have also fabricated individual nanofibers of polyurethane and nylon-6. Thermoplastic polyurethane (PU) and nylon-6 are two of the most widely used polymers because of their excellent properties. Electrospun nanocomposite mat of PU and nylon-6 may exhibit properties shown by both individual polymers and through this combination becomes a new material with improved mechanical properties, thus we have also fabricated a PU/nylon-6 composite by using a modified electrospinning technique utilizing two nozzles with controllable angle between them, with both nozzles placed at one side of the collector. In this paper, we report an investigation of the physical and mechanical properties of nanofibers and nanofiber/film composites fabricated by electrospinning or dip-coating, or a combination of both techniques with the target application of cover of non-vascular stents.

Materials and Method

Materials

The polymers in this study consisted of silicone (Nusil Silicone Technology), thermoplastic polyurethane (Lubrizol Advanced Materials, Inc.), and nylon-6 (Kolon Industries, Inc.). N,N dimethylformamide (DMF) and methyl ethyl ketone (MEK) were purchased from Showa Chemical Co., Ltd., Japan and Junsei, Japan, respectively. Formic acid was received from OCI Co., Ltd. Korea and xylene was received from MITech, Korea. In the present study, all reagents were used without any further purification.

Solution Preparation

Polyurethane and nylon-6 pellets were pre-dried for at least 3 h in an oven at 80 °C prior to dissolution in solvents. PU pellets (10 wt%) was dissolved in DMF/MEK (45/45 wt%) solution; nylon-6 (20 wt%) in formic acid; and silicone (15 wt%) in xylene. All polymers were dissolved in their respective solvents by magnetic stirring at room temperature for 12-15 h.

Electrospinning of Nanofibers

Figure 1(a) shows an electrospinning system used in the present study. It was composed of a high voltage power supply (30 kV, 2 mA, NanoNC, Korea), a robot system controlled by LabVIEW 9.0 program, a syringe, and a grounded cylindrical collector rotating at 50 rpm. The cylindrical collector (d = 20 mm) was oriented horizontally and was located 50 mm away from the spinneret. The spinneret was placed on a robot system that constantly moved laterally, back and forth on its axis for a total distance of 70 mm during electrospinning. A high voltage of 10-28 kV was applied and an electrospun polymer volume of 6 ml was used for all tests. Only PU and nylon-6 were used for electrospinning as it was very difficult to do electrospinning of silicone. Figure 1(b) shows a side-by-side two nozzle electrospinning set-up. A PU/nylon-6 polymer composite was also prepared by electrospinning PU and nylon-6 from two different spinnerets positioned side-by-side to each other. The angle between the spinnerets was 80 ° and the linear distance between the two tips was 40 mm. Both spinneret tips were 50 mm away from the rotating cylindrical collector. Two power supplies were used for the side-by-side configuration. The voltages for PU and nylon-6 were maintained at 10-15 kV and 20-28 kV, respectively. Electrospinning was carried out at room temperature, and the humidity of the chamber was maintained at 20-30 %. The electrospun nanofibers were dried at 80 °C for 24 h after electrospinning. Figure 2(a) shows a dried electrospun nanofiber mat.

Dip-coating and Electrospinning

Only silicone (15 wt%) was used as the polymer for dip-coating. Dip-coating was done by manually applying silicone

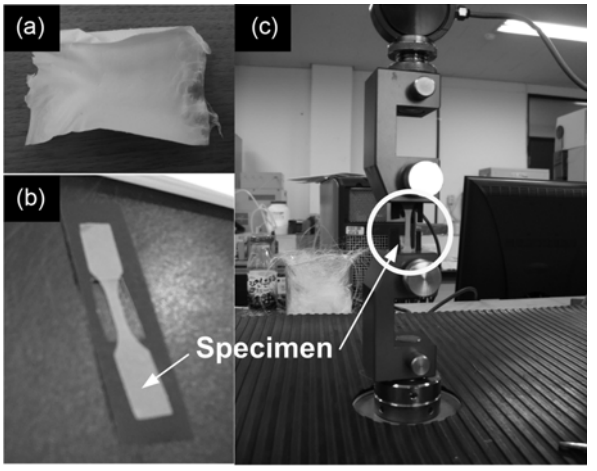

Figure 2. (a) Electrospun nanofiber mat after drying in oven at 80 °C, (b) dog-bone specimen attached on a paper frame for tensile test, and (c) positioning of specimen on a bench-type tensile tester.

solution onto a rotating cylindrical collector at 50 rpm using a syringe at a volume of 5 m*l* prior to electrospinning. Right after silicone was applied onto the collector, the silicone was dried for 5 or 150 min before nanofibers of polyurethane, or nylon-6 were electrospun to the dried/semi-dried silicone film. The resulting nanofiber/film composites were dried for 24 h at 80 °C in a dry oven.

Characterization

The samples were prepared by: (a) dip-coating only, (b) electrospinning only, and (c) combination of dip-coating and electrospinnning. The morphological properties of all samples were observed using SEM (Hitachi X-650, Japan). The diameter distribution of the nanofibers was measured using ImageJ software (NIH, USA) based from the SEM images and the average of at least 50 fiber measurements was used. X-ray diffraction spectra were obtained using multi-purpose high performance X-ray diffractometer (PANalytical, Netherlands). FTIR spectra of neat nanofiber and film, and composite nanofiber/film were measured using Spectrum GX (Perkin Elmer, USA) at a signal resolution of 1 cm^{-1} and a minimum of 16 scans was obtained and averaged within the range of 400-4000 cm^{-1}. The tensile properties of the composite films were obtained using an Instron Bench-type Tensile Tester (LR5K Plus, Lloyd Instruments, 100 N load limit) (see Figure 2(c)) using a dog-bone specimen based from ASTM D882-10 (Standard Test Method for Tensile Properties of Thin Plastic Sheeting). The specimens were fixed on a paper frame by taping both ends of the specimen (see Figure 2(b)). The crosshead speed was 10 mm/min and 5-10 specimens were tested for each sample. The thickness of the specimens were measured using a digital microcaliper (Mitutoyo Absolute, Mitutoyo Corp., Japan) with an accuracy of ±0.5 μm by getting the average value of at least 3 measurements.

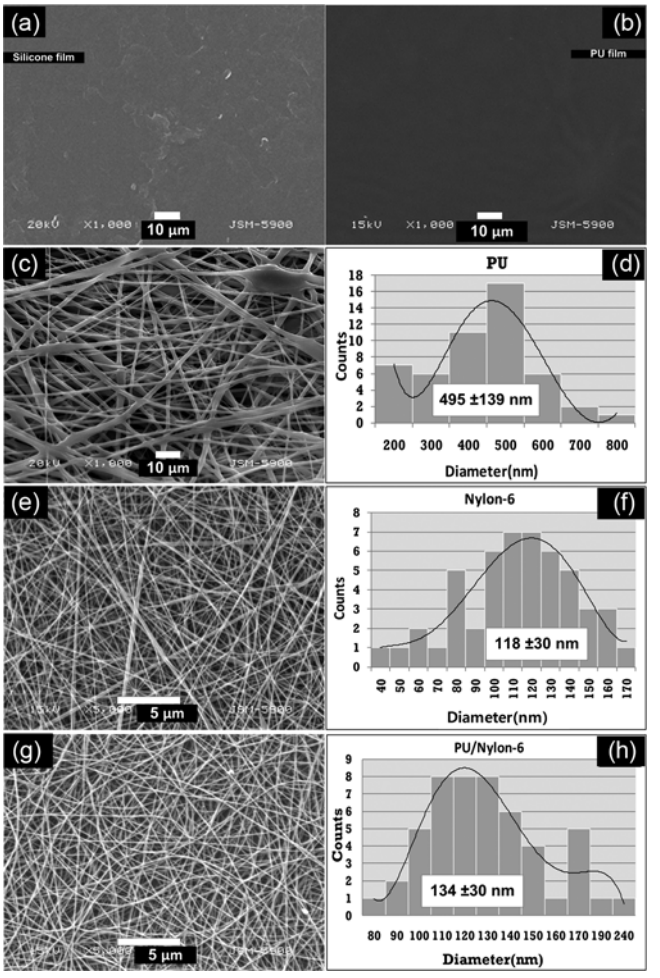

Figure 3. Surface morphology of pure dip-coated (a) silicone, (b) polyurethane films and electrospun nanofibers of pure, (c) polyurethane, (e) nylon-6, and (g) polyurethane/nylon-6 composite. The fiber diameter distributions for PU, nylon-6, and PU/nylon-6 composite are shown in (d), (f), and (g), respectively.

Results and Discussion

Surface Morphology and Fiber Diameter Distribution

Figure 3 shows the SEM images of the fabricated PU and silicone films, and the electrospun pure PU, nylon-6, and PU/nylon-6 composite with their corresponding fiber diameter distributions. Silicone and PU films (Figures 3(a) and (b)) fabricated by dip-coating show non-porous uniform surface. The electrospun nanofibers (Figures 3(c), (e), and (g)) on the other hand show highly-porous, ultra fine matrix of interlocking fibers in the nanometer range, and randomly-ordered non-woven mats. PU nanofibers show generally bigger fiber diameters as compared to nylon-6 and PU/nylon-6 composite. Some beads were formed on PU nanofiber, which could be attributed to relatively low viscosity or short distance between the spinneret tip and the collector [27,28]. The PU and nylon-6 nanofibers give more straight

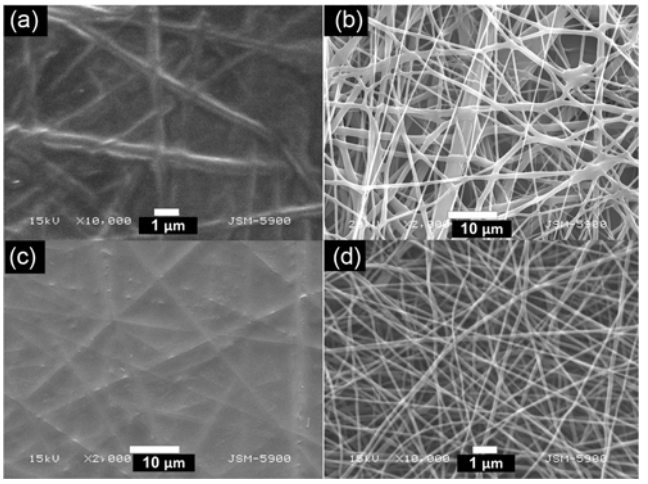

Figure 4. Surface morphology of polyurethane (a, b) and nylon-6 (c, d) electrospun nanofiber/film composites for silicone film drying time of 5 min (a, c) and 150 min (b, d).

yet randomly-oriented fibers (Figures 3(c) and (e)) while PU/nylon-6 composite (Figure 3(g)) shows very random, curvy fibers, with relatively uniform fiber sizes. It should be noted that pure PU and nylon-6 nanofibers were electrospun using a single spinneret oriented perpendicular to the flat collector while the PU/nylon-6 composite used two spinnerets with an angle of 80 ^{o} between them. The distance between the tip of the spinneret/s was maintained at 50 mm for all configurations. The fiber diameter distributions of PU, nylon-6 and PU/nylon-6 are shown in Figures 3(d), (f), and (h) (respective insets show the fiber diameter averages). The average diameter of PU, nylon-6, and PU/nylon-6 nanofibers were 496±139 μm, 118±30 μm, and 134±30 μm, respectively. It is a nature of electrospun nanofibers to have uneven fiber diameter distribution due to bending and axisymmetrical instabilities [23,29]. In the case of PU/nylon-6 composite, its spinneret configuration (i.e., 80 ^{o} between two spinnerets) could have made more bending instabilitites thereby producing more curly and wavy non-woven nanofibrous mats.

Figure 4 shows the SEM images of PU/silicone or nylon-6/silicone nanofiber/film composites. The silicone dip-coated films were either dried for 5 or 150 min before electrospinning the PU or nylon-6 nanofibers onto the silicone film. For both PU/silicone and nylon-6/silicone composites with silicone drying of 5 min show embedded nanofibers inside the silicone film. The morphologies of Figure 4(a) and (c) suggest good nanofiber/silicone interfacial adhesion [23]. When silicone film was dried at ambient temperature before electrospinning nanofibers, the resulting composite (see Figures 4(b) and (d)) show very distinct nanofiber formations. The nanofiber and film in this case give two distinct layers for nanofiber and film, thus suggesting poor interfacial adhesion. The effect of these interfacial layer adhesions could be clearly seen in the mechanical properties of the resulting composites in Figure 7.

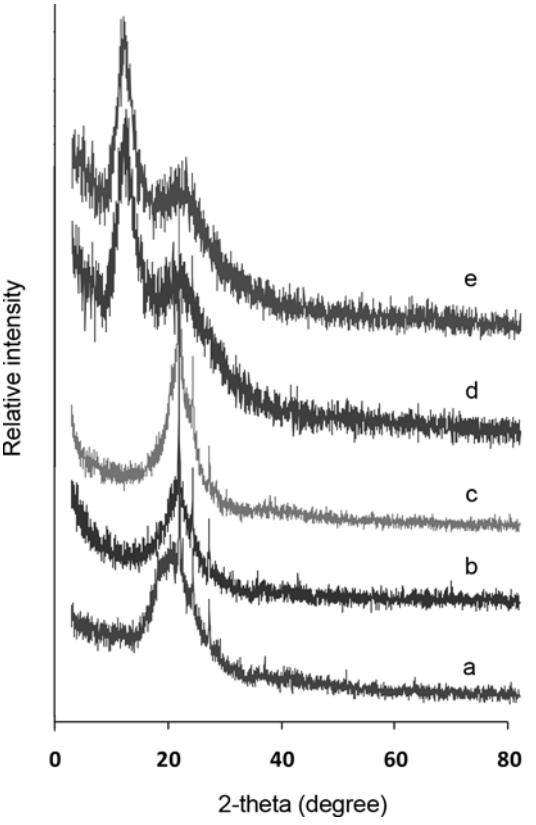

Figure 5. XRD spectra of electrospun nanofibers: (a) PU, (b) nylon-6, (c) PU/nylon-6 composite, and nanofiber/silicone film (5 min drying) composites of; (d) PU/silicone, and (e) nylon-6/silicone.

XRD and Infrared Spectroscopy

The crystalline structures of the electrospun nanofibers and dip-coated films were characterized by XRD and the results are shown in Figure 5. One or two broad peaks in the XRD results indicate a typical pattern for low crystalline material [30]. The peak at $2\theta = 20^{o}$ in Figure 6(a) corresponds to the crystallization of the soft segment of PU [31]. The XRD spectra of nylon-6 (Figure 5(b)) shows peaks at 21 ^{o} (200) and 24 ^{o} (002), which are attributed to the α crystalline structure of nylon-6 [32]. In Figures 5(d) and (e), the existence of silicone polymer is evidenced by the broad peaks between 10 ^{o} and 15 ^{o} [33], and peaks at 20 ^{o} and 21 ^{o} correspond to PU and nylon-6, respectively.

Figure 6 shows the FTIR spectra of the electrospun nanofibers and nanofiber/film composites. The broad peaks at 3420-3480 cm^{-1} are attributed to the presence of moisture on the surface at different modes and for the stretching of -OH. The characteristic peaks of PU nanofibers can be assigned as: 2925 cm^{-1} (CH_2 asymmetric vibration); 2857 cm^{-1} (CH_3 symmetric vibrations) [31]; 1735 cm^{-1} (free C=O); 1700 cm^{-1}

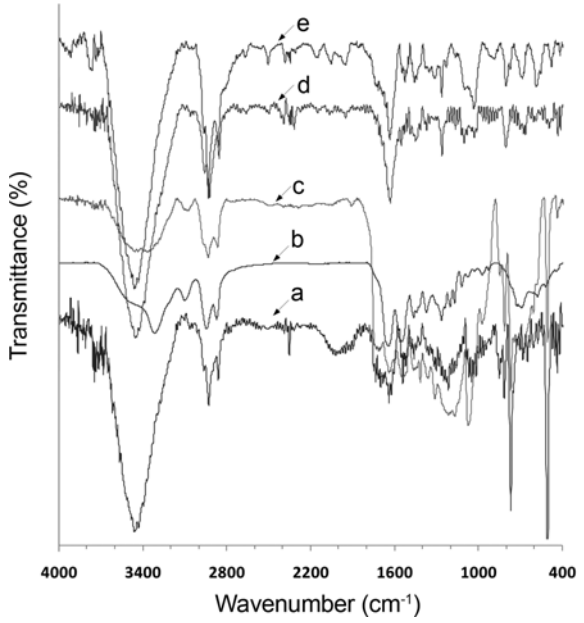

Figure 6. FTIR spectra of electrospun nanofibers: (a) PU, (b) nylon-6, (c) PU/nylon-6 composite and nanofiber/silicone film (5 min drying) composites of; (d) nylon-6/silicone, and (e) PU/silicone.

Table 1. Tensile strength and percentage strain at break of electrospun nanofibers, dip-coated films, and nanofiber/film composites

Material	Tensile strength (MPa)	Strain at break (%)
Dip-coated PU film	59.0±6.5	841±68
Dip-coated silicone film	3.9±0.7	2063±518
Polyurethane nanofiber	7.8±1.5	430±140
Nylon-6 nanofiber	5.7±2.2	41±9
PU/nylon-6 nanofiber	11.5±0.6	73±11
Silicone film (5 min)/PU nanofiber	8.2±1.0	1941±381
Silicone film (150 min)/PU nanofiber	2.9±0.5	942±435
Silicone film (5 min)/nylon-6 nanofiber	9.3±0.3	2289±236
Silicone film (150 min)/nylon-6 nanofiber	3.4±0.4	834±283

(C=O bond); 1534 cm^{-1} (urethane amide II); 1073 cm^{-1} (C(O)-O-C stretching of the hard segment; and 820 cm^{-1} (bending vibration in benzene ring) [34]. For nylon-6, the following are the assigned bands: 2934 cm^{-1} (CH_2 asymmetric stretching); 2870 cm^{-1} (CH_2 symmetric stretching); 1376 cm^{-1} (amide III + CH_2 swagging); 1270 cm^{-1} (CH_2 twist wag vibration); 1202 cm^{-1} ((amide III + CH_2 swagging); 1538 cm^{-1} (amide II); 1647 cm^{-1} (amide I); and 1081 cm^{-1} (CC stretching). The composite nanofiber mat (Figure 6(c)) showed spectral patterns of both PU and nylon-6, indicating the structural independence of both nanofibers. However, the band at 1538 cm^{-1} (amide II) of pristine nylon-6 was observed to have shifted to lower frequency in composite mats, indicating an

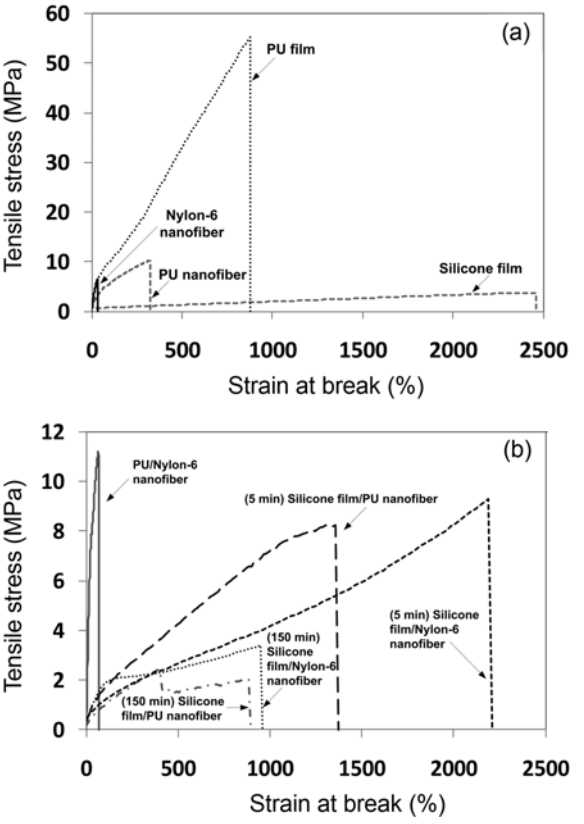

Figure 7. Typical stress-strain relationship of (a) pure polymer electrospun nanofiber and dip-coated films and (b) electrospun nanofiber composite and nanofiber/film composites.

interaction of nylon-6 with PU by means of the formation of stronger hydrogen bond [35]. This change is possible due to the specific interactions that influence the vibrational frequency of functional groups as detected through the FTIR. The following are the bands assigned for characteristic peaks of silicone: 2962 cm^{-1} (CH stretching of CH_3); 1412 cm^{-1} (CH_3 asymmetric deformation of Si-CH_3); 1092 cm^{-1} (Si-O-Si stretching vibrations). Figures 6(c)-(e) show that each component polymer was present for the composite materials, and kept their structural independence [11].

Mechanical Property

The mechanical properties of the nanofibers and composite nanofiber/film are important for biomedical and stent applications. Figure 7 shows the typical stress-strain behavior of the electrospun nonofibers, dip-coated films and composite films. The summary of tensile strength and tensile strain obtained from 5-10 specimens is shown in Table 1. Polyurethane dip-coated film (Figure 7(a)) exhibited the highest tensile strength of 59.0±6.5 MPa from all the fabricated samples in the present study. Silicone film on the other hand had the highest strain at break of 2063 % but low tensile strength (~3.9 MPa). The present mechanical properties of dip-coated polyurethane and silicone films were similar with

the values reported in commercial stent covers. The PU electrospun nanofibers showed much lower mechanical behavior compared to the bulk PU film. This phenomenon is primarily because of the much lower density of the porous PU nanofiber mats and the non-woven, multi-directional orientation of the nanofibers [36]. The PU nanofibers showed better mechanical properties than nylon-6 nanofiber mats. Nylon-6 nanofibers were quite brittle compared to PU nanofibers. The electrospun PU/nylon-6 composite nanofiber by side-by-side electrospinning produced better tensile strength than either of pure PU or nylon-6 nanofibers alone, but it suffered a low tensile strain (see Figure 7(b)). This increased tensile strength of composite mat is attributed to the newly formed hydrogen bonding between PU and nylon-6 molecules as signified in the FTIR spectra (Figure 6(c)). Furthermore, the composite nanofibers showed very random, curvy, and uniform diameter nanofiber morphology. This morphology signifies higher density than their individual pristine mats, which could have helped in increasing its tensile strength. The present electrospun nanofibers were composed of ultrafine, randomly-oriented nanofibers with various diameters and lengths, in which case, delamination and slipping of the fiber during tensile test would have a negative effect on the mechanical strength of the mats [37]. Thus, the present mechanical property results do not necessarily reflect the property of a single nanofiber [20]. The porosity and high surface area-to-volume ratio of a material plays an important factor in the performance of different membranes, adsorbents, etc. [22,38]. High porosity is essential to tissue engineering to mimic extracellular matrix, also as possible drug-delivery sites in the cover of non-vascular stents [11,16]. Shalaby [39] fabricated an electrospun nanofiber-covered drug-eluting stent that could slowly release drug on the target area in the body to help prevent in-stent restenosis, and facilitate the proliferation and adhesion of cells. Kuraishi *et al*. [16] obtained promising results for electrospun PU nanofiber-covered stent to treat cerebral aneurysm. Since stent materials inside the body are constantly exposed to bending and pulsatile conditions, the importance of mechanical properties of the electrospun nanofiber or composite material for stent cover is very obvious [11].

The ideal material for stent cover should have good tensile strength and good flexibility. Silicone has high tensile strain but low tensile strength. Polyurethane and nylon-6 have better tensile strengths than silicone but have several magnitudes lower tensile strains. In order to avail the individual mechanical properties of the polymers, composite materials were fabricated by combining either electrospun PU or nylon-6 with silicone film. The silicone was dried for 5 or 150 min before nanofibers were electrospun. Figure 7(b) shows that a semi-dried silicone film (i.e., dried for 5 min) combined with electrospun nanofibers produced much higher tensile strengths and strains than those of silicone dried for 150 min. From the SEM images, one could see that 5 min drying of silicone embedded the nanofibers into the film, thus giving good interfacial adhesion between two polymers resulting into better mechanical property. The tensile strength and strain of nylon-6/silicone (5 min drying) composite were 9.3 ± 0.3 MPa and 2289 %, respectively. These show increase in tensile strength of 63 % from pure nylon-6 nanofiber, and 135 % from pure silicone film, without sacrificing its flexibility. The PU/silicone (5 min drying) also showed better mechanical performance (i.e., 8.2 ± 1 MPa, and 1941 %) than their individual fabrication of nanofiber and film. It is interesting to note that even though the pure PU nanofiber had better mechanical property than pure nylon-6 nanofiber, but when combined with silicone film, nylon-6/silicone composite produced much better mechanical performance than PU/silicone in the present study. This can be explained by looking at the morphologies (see Figure 3) of PU and nylon-6 nanofibers. The more uniform and much smaller-sized nylon-6 nanofibers could have much more surface area than the bigger and less uniform PU nanofibers for silicone to have good interfacial adhesion between the two polymers. Good interfacial adhesion and bonding is a requisite to have an effective load transfer of reinforcing fillers to the host matrix [23]. The distinct layers of nanofiber and film in the silicone dried at 150 min for both PU and nylon-6 could have resulted in poor interfacial adhesion, thus the mechanical properties also show poor results.

One advantage of using electrospun nanofiber in the outer layer of a stent is its uniformity. Dip-coating alone presents high tendency for non-uniform layer. A thin and uniform membrane, high tensile strength, and high stretching possibility pose big advantages for stent application. It presents easier loading and unloading to and from the introducer with longer extension, and poses lesser friction so that there is lesser tendency for the cover to be torn. Electrospun nanofibers are promising in this regard. The addition of filler material is one way of improving the physical and mechanical properties of nanofibers like the addition of carbon nanotubes.

Conclusion

In this study, silicone, polyurethane and nylon-6 polymers were used to fabricate nanofibers by electrospinning, and nanofiber/film composite by electrospinning and dip-coating. The resulting nanofibers and composite materials were characterized by SEM, XRD, FTIR, and tensile test. The present findings show that reinforcing the dip-coated silicone film with electrospun nanofiber could improve its mechanical property. The optimum result was obtained at silicone film (5 min drying)/nylon-6 nanofiber composite showing 63 % increase in tensile strength compared to nylon-6 nanofiber alone, with very good stretchability. The present nanofiber/film composite material has promising

applications for stent cover, having good mechanical strength and strain. Further investigations are on-going for the incorporation of different filler materials like carbon nanotube, in conjunction with the use of side-by-side and coaxial electrospinning to improve the physical and mechanical properties of composites for biomedical and stent applications.

Acknowledgments

This research was supported by a grant from the Korean Ministry of Education, Science and Technology through the Regional Core Research Program/Center for Healthcare Technology Development (Project no. 1345110369) and partially by a grant from the Business for International Cooperative Research and Development between Industry, Academy and Research Institute funded by the Korean Small and Medium Business Administration (Project no. 00042172-1).

References

1. H. Zhao, J. Van Humbeeck, J. Sohier, and I. de Scheerder, *Prog. Biomed. Res*., **8**, 70 (2003).
2. P. Sojitra, C. Engineer, A. Raval, D. Kothwala, A. Jairwala, H. Kotadia, S. Adeshara, and G. Mehta. *Trends Biomater. Artif. Organs*., **23**, 55 (2009).
3. N. Nagai, Y. Nakayama, S. Nishi, and M. Munekata, *J. Artif. Organs*, **12**, 61 (2009).
4. S. Moon, S. G. Yang, and K. Na, *Biomaterials*, **32**, 3603 (2011).
5. B. Thierry, Y. Merhi, J. Silver, and M. Tabrizian, *J. Biomed. Mater. Res. A*, **75**, 556 (2005).
6. Y. Nakayama, S. Nishi, H. Ueda-Ishibashi, and T. Matsuda, *J. Biomed. Mater. Res. A.*, **64**, 52 (2003)
7. Y. Chen, J. Lin, Y. Fei, H. Wang, and W. Gao, *Fibers Polym*., **11**, 1128 (2010).
8. H. Isayama, Y. Komatsu, T. Tsujino, N. Sasahira, K. Hirano, N. Toda, Y. Nakai, N. Yamamoto, M. Tada, H. Yoshida, Y. Shiratori, T. Kawabe, and M. Omata, *Gut*, **53**, 729 (2004).
9. S. Thurnher, J. Lammer, M. Thurnher, F. Winkelbauer, O. Graf, and R. Wildling, *Cardiovasc. Intervent. Radiol.*, **19**, 10 (1996).
10. M. Bezzi, A. Zolovkins, V. Cantisani, F. Salvatori, M. Rossi, F. Fanelli, and P. Rossi, *J. Vasc. Interv. Radiol.*, **13**, 581 (2002).
11. R. Chen, C. Huang, Q. Ke, C. He, H. Wang, and X. Mo, *Colloid Surface B*, **79**, 315 (2010).
12. M. Gu, K. Wang, W. Li, C. Qin, J. J. Wang, and L. Dai, *Fiber Polym.*, **12**, 65 (2011).
13. R. Gopal, S. Kaur, Z. Ma, C. Chan, S. Ramakrishna, and T. Matsuura, *J. Mem. Sci*., **281**, 581 (2006).
14. C. Shao, H. Y. Kim, J. Gong, B. Ding, D. R. Lee, and S. J. Park, *Mater. Lett.*, **57**, 1579 (2003).
15. H. Fong and D. H. Reneker in "Structure Formation in Polymeric Fibers" (D. R. Salem Ed.), pp. 225-246, Hanser, Munich, 2001.
16. K. Kuraishi, H. Iwata, S. Nakano, S. Kubota, H. Tonami, M. Toda, N. Toma, S. Matsushima, K. Hamada, S. Ogawa, and W. Taki, *J. Biomed. Mater. Res. A*, **88B**, 230 (2009).
17. M. W. Frey and L. Li, *J. Eng. Fibers Fabr.*, **2**, 31 (2007).
18. H. G. Kim and J. H. Kim, *Fiber Polym.*, **12**, 602 (2011).
19. C. Tang and H. Liu, *Composites Part A*, **39**, 1638 (2008).
20. Z. M. Huang, Y. Z. Zhang, M. Kotaki, and S. Ramakrishna, *Compos. Sci. Technol.*, **63**, 2223 (2003).
21. S. Lingaiah, K. N. Shivakumar, and R. L. Sadler, *Proceedings of 49th AIAA/ASME/ASCE/AHS/ASC Structures,* Schaumburg, IL 1-13, 2008.
22. P. Lu and B. Ding, *Recent Patents on Nanotech.*, **2**, 169 (2008).
23. H. Liao, Y. Wu, M. Wu, and H. Liu, *Polym. Compos*., 838 (2011).
24. D. Shi, J. Lian, P. He, L. M. Wang, F. Xiao, L. Yang, M. J. Schulz, and D. B. Mast, *Appl. Phys. Lett*., **83**, 5301 (2003).
25. M. Nogi and H. Yano, *Adv. Mater*., **20**, 1849 (2008).
26. S. Lin, Q. Cai, J. Ji, G. Sui, Y. Yu, X. Yang, Q. Ma, Y. Wei, and X. Deng, *Compos. Sci. Technol.*, **68**, 3322 (2008).
27. M. M. Demir, I. Yilgor, E. Yilgor, and B. Erman, *Polymer*, **43**, 3303 (2002).
28. G. Eda, J. Liu, and S. Shivkumar, *Mat. Lett.*, **61**, 1451 (2007).
29. D. H. Reneker, A. L. Yarin, H. Fong, and S. Koombhongse, *J. Appl. Phys*., **87**, 4531 (2000).
30. R. C. M. Dias, A. M. Goes, R. Serakides, E. Ayres, and R. L. Orefice, *Mat. Res.*, **13**, 211 (2010).
31. S. Guo, C. Zhang, H. Peng, W. Wang, and T. Liu, *Compos. Sci. Technol.*, **71**, 791 (2011).
32. V. Vasanthan and D. R. Salem, *J. Polym. Sci. Pol. Phys.*, **39**, 536 (2001).
33. U. M. Rao, S. S. M. S. Abdul Majeed, C. Venkataseshaiah, and R. Sarathi, *Bull. Mater. Sci.*, **25**, 473 (2002).
34. A. S. Khan, Z. Ahmed, M. J. Edirisinghe, F. S. L. Wong, and I. U. Rehman, *Acta Biomat*, **4**, 1275 (2008).
35. H. R. Pant, M. P. Bajgai, C. Yi, R. Nirmala, K. T. Nam, W. Baek, and H. Y. Kim, *Colloid Surf. A: Physico. Eng. Asp.*, **370**, 87 (2010).
36. A. Pedicini and R. J. Farris, *Polymer*, **44**, 6857 (2003).
37. S. Soliman, S. Pagliari, A. Rinaldi, G. Forte, R. Fiaccavento, F. Pagliri, O. Franzese, P. M. Minieri, D. Nardo, S. Licococia, and E. Traversa, *Acta Biomaterialia*, **6**, 1227 (2006).
38. W. He, T. Yong, W. E. Teo, Z. Ma, and S. Ramakrishna, *Tissue Eng*., **11**, 1574 (2005).
39. S. W. Shalaby, US 2006195142 (2006).